Supplementary Figure Legends

Supplementary Figure 1. Metabolic stress induces intracellular hypoxia and HIF-2α expression in Min6 cells. (**A**) IHC analysis of insulin (green) and HIF-2α (magenta) expression in pancreatic islets of tamoxifen-treated WT and HIF-2α βKO mice fed HFD (ad libitum). Even with increased camera exposure, we did not detect significant amount of nuclear HIF-2α in the beta cells of HIF-2α βKO mice. (**B**) Relative HIF-1α and HIF-2α band intensity normalized to Actin in Figure 1E and two additional independent repeat experiments with the same experimental conditions. (**C**) Pimonidazole adduct formation was assessed using immunocytochemistery analysis of Min6 cells incubated in low (2.8 mM) and high (16.8 mM) glucose conditions in the presence or absence of 100 μM palmitic acid for 24h. Cells were treated with 10 μM pimonidazole (Hypoxyprobe-1 plus; Hypoxyprobe Inc, Burlington, USA) 30 min before harvesting the cells. Fixed cells were stained with FITC-conjugated anti-pimonidazole adduct antibodies (green) and images were acquired using confocal microscopy (20X). (**D**) Relative pimonidazole adduct staining intensity was normalized by the number of nuclei (DAPI-positive) in a given area of images from the panel C experiments. Results were plotted and presented. Grey bars, 2.8 mM glucose; open bars, 16.8 mM glucose; PA, palmitic acid. Throughout, **P*<0.05, ***P*<0.01, and *****P*<0.001. All data are presented as mean +/- SEM. Statistical analysis was performed by the 2-way ANOVA with Tukey's multiple comparison tests.

Supplementary Figure 2. Inducible depletion of beta cell HIF-2α in adult mice does not affect GSIS and glucose tolerance on NCD. H2βKO^{MIP}, H2βKO^{PDX1}, Cre$^{-/-}$:*Hif2a*$^{fl/fl}$ littermate control, and age-matched MIP-CreERT mice were fed NCD. At the age of 20 weeks, mice were

fed a tamoxifen-containing NCD for 1 week. At the age of 21 week, diet was switched back to NCD. After 2 weeks of recovery on NCD, mice were subjected to OGTTs. (**A**) Schematic representation of experimental time line. (**B-D**) mRNA (B and D) and protein (C) expression of *Hif1a* and *Hlf2a* in the islets from H2βKO^{MIP}, *Cre*$^{-/-}$:*Hif2a*$^{fl/fl}$ littermate control, and age-matched MIP-CreERT mice or H2βKO^{PDX1} and Cre$^{-/-}$:*Hif2a*$^{fl/fl}$ littermate control mice (n= 5 mice per group in panel B and D and n=3 mice in panel C). Set 1~3 results in panel C represents three independent experiments using islets from one WT and one KO mice in each. To induce HIF-2α expression, isolated islets were incubated in a normoxia (21% oxygen; Norm) or hypoxia (1% oxygen; Hypo) condition for 6 h and subjected to Western blot analyses. (**E-F**) body weight in H2βKO^{MIP}, Cre$^{-/-}$:*Hif2a*$^{fl/fl}$ littermate control, and age-matched MIP-CreERT mice (E; n= 6, 7, and 6 mice per group) or in the islets from H2βKO^{PDX1} and Cre$^{-/-}$:*Hif2a*$^{fl/fl}$ littermate control mice (F; n= 18 and 44 mice per group). (**G**) Oral glucose tolerance tests (n= 6, 7, and 7 mice per group). (**H**) Plasma insulin levels during OGTT in panel G mice. (**I**) Plasma C-peptide levels during OGTT in panel G mice. (**J**) Oral glucose tolerance tests (n= 9 and 9 mice per group). (**K-R**) Islet morphology analysis in pancreatic sections of HFD MIP-CreERT (K), H2βKO^{MIP} (K), *Cre*$^{-/-}$:*Hif2a*$^{fl/fl}$ (L), and H2βKO^{PDX1} (L) mice after immune-staining with anti-insulin and anti-glucagon antibodies. More than four mice were used for the analysis of islet morphology in each group and representative figures are shown. (**M, O**) Relative beta cell mass (n= 5, 3, and 4 mice per group in panel M and 5 and 4 mice in panel O). (**N**, **P**) Islet number per pancreatic section area (n= 4, 3, and 4 mice per group in panel N and 4 and 4 mice in panel P). (**Q**, **R**) Pancreatic mass (n= 7, 5, and 4 mice per group in panel Q and 7 and 4 mice in panel R). (**S**) *Ex vivo* static GSIS tests in isolated islets (n=5, 5, 10, and 10 mice per group). Throughout, **P*<0.05. All data are presented as mean +/- SEM. Statistical analysis was performed by the 2-way ANOVA with Tukey's multiple comparison tests.

Supplementary Figure 3. Analysis of primary islets from HFD HIF-2α beta cell KO and control mice. (**A**) Time course changes in body weight in WT and βKO^{MIP} mice during 12 weeks of HFD. (**B**) Area under the curve (AUC) during OGTTs in Figure 2D. (**C**) Intra-islet insulin content in HFD MIP-CreERT, H2βKO^{MIP}, *Cre*$^{-/-}$:*Hif2a*$^{fl/fl}$, and H2βKO^{PDX1} mice (n=5, 5, 10, and 10 mice per group). (**D**) *Ex vivo* static GSIS tests in isolated islets (n=45, 24, and 24 wells per group for WT islets and 24, 12, and 12 wells per group for KO islets). (**E**) Islet number per pancreatic section area in HFD H2βKO^{MIP}, *Cre*$^{-/-}$:*Hif2a*$^{fl/fl}$ littermate control mice, and age-matched MIP-CreERT mice (n= 7, 2, and 7 mice per group). (**F**) Islet number per pancreatic section area in HFD H2βKO^{PDX1} and *Cre*$^{-/-}$:*Hif2a*$^{fl/fl}$ littermate control mice (n= 9 and 8 mice per group). (**G**) Average beta cell size was calculated by dividing total insulin-positive beta cell area by the number of beta nuclei in each islet (n= 7, 2, 4, and 8 mice per group). (**H**) The proportion of alpha cell area was calculated by dividing total glucagon-positive alpha cell area by total islet area (alpha cell + beta cell area) in each of the islets (n= 7, 2, 4, and 8 mice per group). (**I**) The ratio of alpha:beta cells was calculated by dividing the number of glucagon-positive cell nuclei by the number of insulin-positive cell nuclei (n= 7, 2, 4, and 8 mice per group; two islets were randomly selected from each mouse section and the alpha:beta ratios in the two islets were averaged. This average ratio was considered as the representative alpha:beta ratio of each mouse). Throughout, **P*<0.05 and ***P*<0.01. All data are presented as mean +/- SEM. Statistical analysis was performed by unpaired t-test (B) or the 2-way ANOVA with Tukey's multiple comparison tests.

Supplementary Figure 4. *Hif1a* and *Arnt* expression, Arn1-HIF-1α interaction, and/or ROS levels in HIF-2α or HIF-1α KD Min6 cells. (**A**) *Hif1a* expression in Min6 cells transfected with mock or *Hif2a*-specific siRNAs. 24h after transfection, cells were incubated in low (2.8 mM) or high (16.8 mM) glucose media for 48h. (**B**) Western blot analysis of HIF-1α and HIF-2α

expression in control and HIF-2α KD Min6 cells incubated in low or high glucose media for 24h in the presence or absence of MitoTEMPO. Results from two additional independent experiments performed in the same condition with Figure 3C are shown. These results were used to plot relative HIF-1α and HIF-2α expression in Figure 3C (right). (**C**) Western blot analysis of HIF-1α and HIF-2α expression in control and HIF-2α KD Min6 cells incubated in low or high glucose media for 24h. Results from three independent experiments are shown. The relative ratio of HIF-1α to Actin expression was calculated and presented on the right. (**D**) Immunoprecipitation (IP) Western blot analysis of Arnt-associated HIF-1α and HIF-2α expression in control and HIF-2α KD Min6 cells. Min6 cells were incubated in 2.8 mM or 16.8 mM glucose media for 24h. Total lysates were prepared and subjected to IP experiments with anti-Arnt antibody (Novus, Cat. #NB100-124SS)-coated or control beads (Thermo, Cat. #10003D). Samples were analyzed by Western blots with anti-Arnt, anti-HIF-1α, and anti-HIF-2α antibodies. (**E**) Mitochondrial ROS levels in Min6 cells transfected with mock or *Hif2a*-specific siRNAs. 24h after transfection, cells were incubated in low (2.8 mM) or high (16.8 mM) glucose media for 24h. (**F**) Cytosolic ROS levels in Min6 cells transfected with mock or Hif2a-specific siRNAs. 24h after transfection, cells were incubated in low (2.8 mM) or high (16.8 mM) glucose media for 24h. (**G**) Immuno-fluorescence cytochemistry analysis of Tom20-positive area in control and HIF-2α KD Min6 cells incubated in low or high glucose media in the presence or absence of MitoTEMPO. Relative Tom20-positive area was calculated and plotted in Figure 5F. (**H**) Intracellular ROS levels. Min6 cells were transfected with mock or *Hif1a*-specific siRNAs. 24h later, cells were incubated in high glucose (16.8 mM) media for another 24 h in the presence or absence of PHDi. Throughout, **P*<0.05, ***P*<0.01, and *****P*<0.001. All data are presented as mean +/- SEM. Statistical analysis was performed by the 2-way ANOVA with Tukey's multiple comparison tests.

Supplementary Figure 5. DNA sequence motif analysis for the presence of putative hypoxia response element (HRE) in human and mouse *SOD2* and *CAT* gene promoter regions. DNA sequences 2 kb upstream from the transcription start site of human and mouse *SOD2* and *CAT* genes were used to identify putative HREs using a web-based open-access DNA sequence motif analyzing algorithm, JASPAR. In this analysis, each of the motifs of candidate TF binding sites were assigned scores by the position weight matrix for the given sequence (Doi: 10.1093/nar/gkz1001)

Supplementary Figure 6. Schematic model of how HIF-2α supports beta cell compensation in obesity.

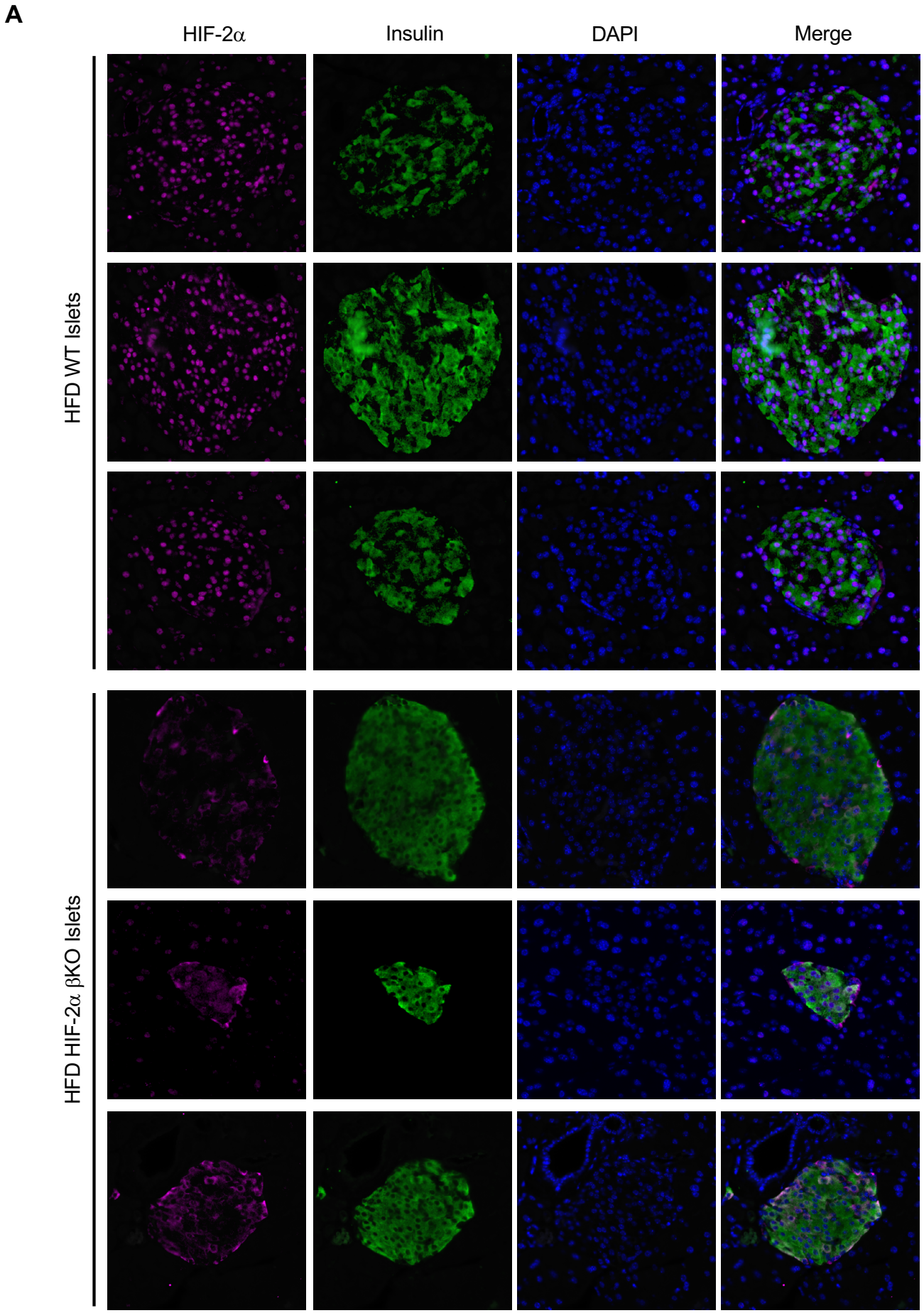

Supplementary Figure 1

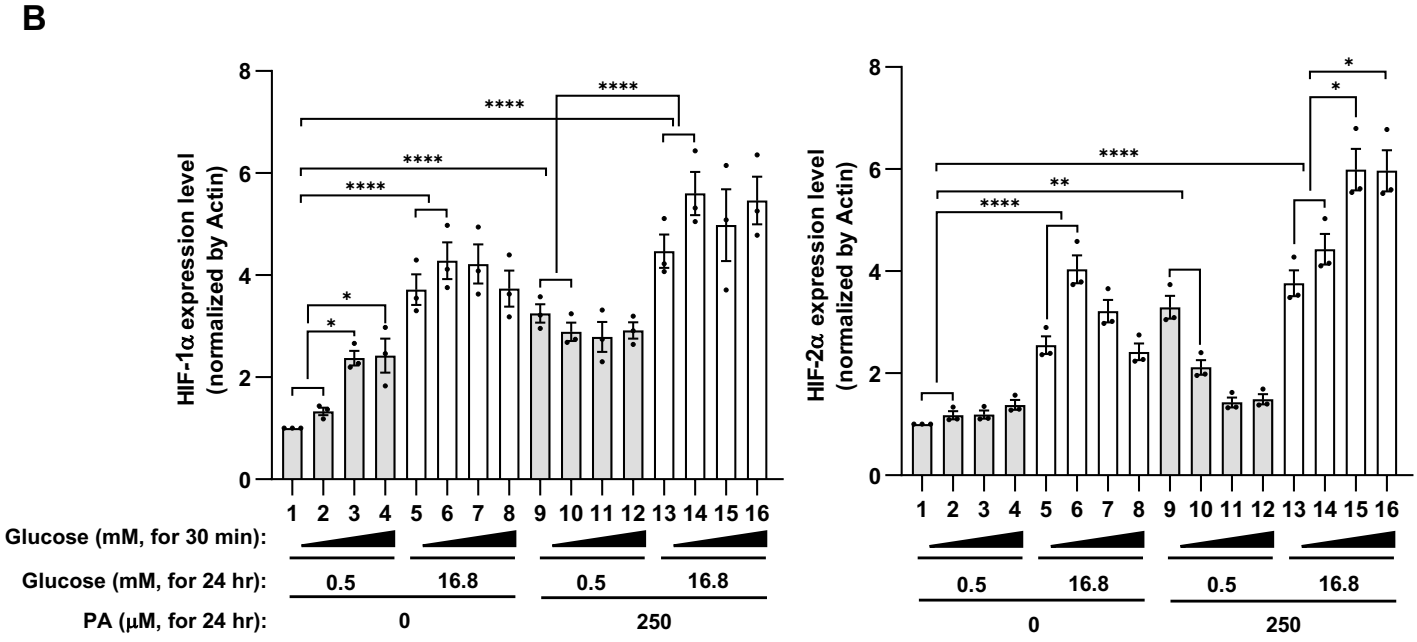

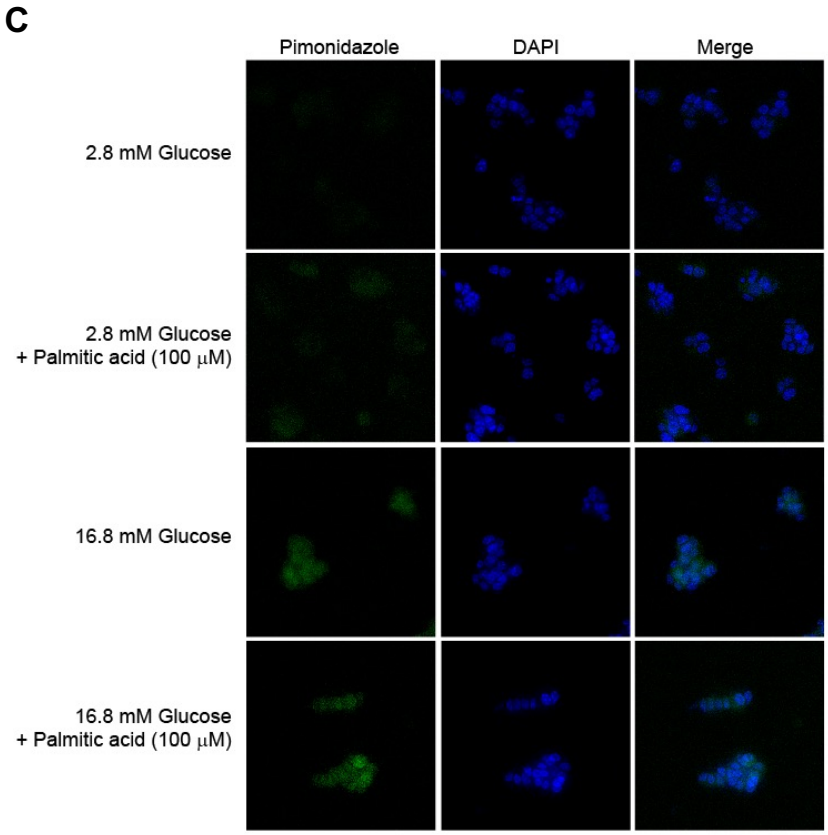

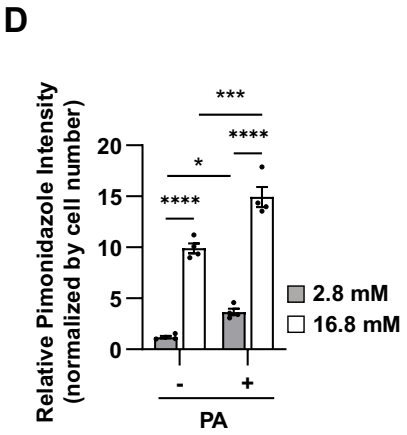

Supplementary Figure 1

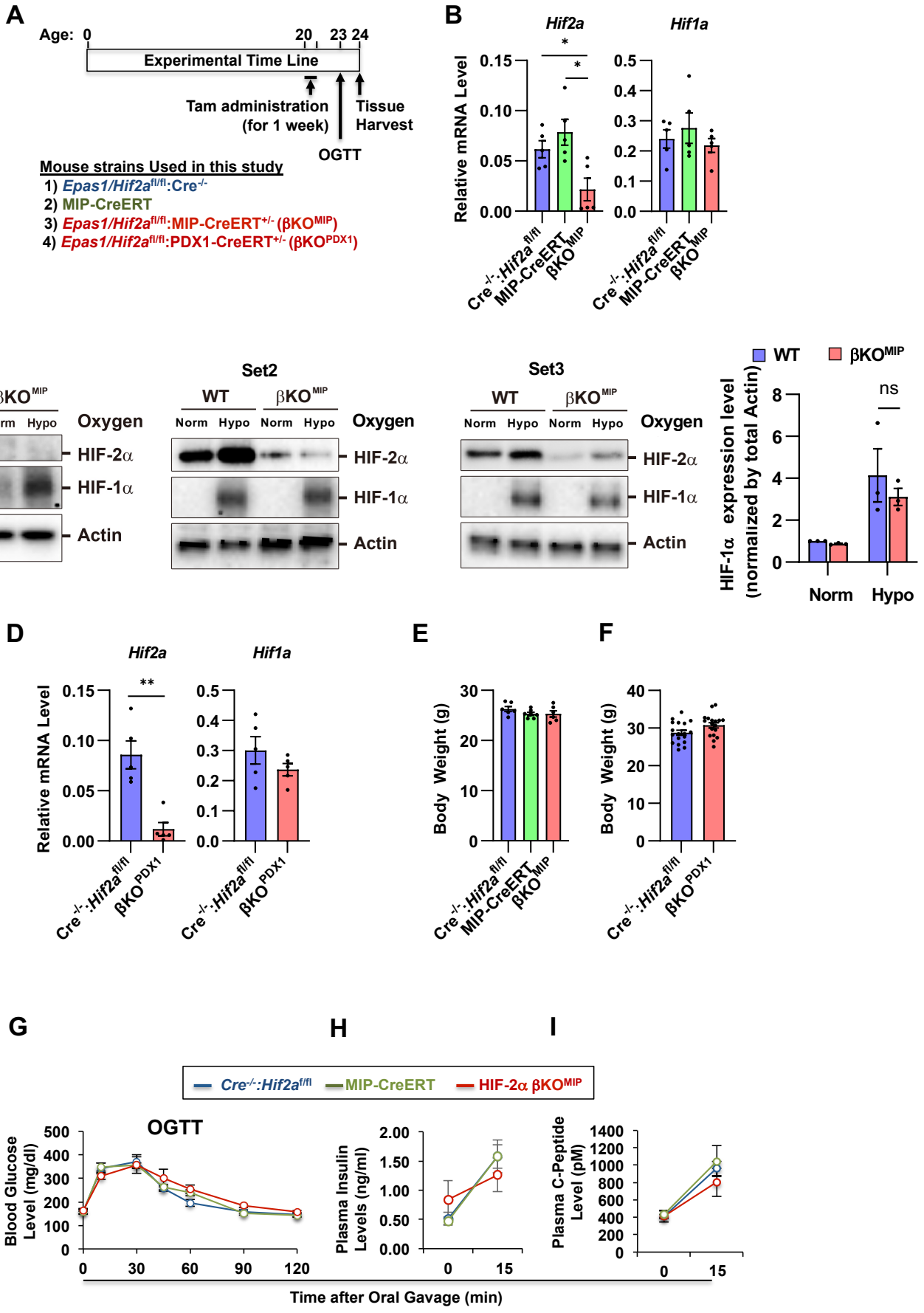

Supplementary Figure 2

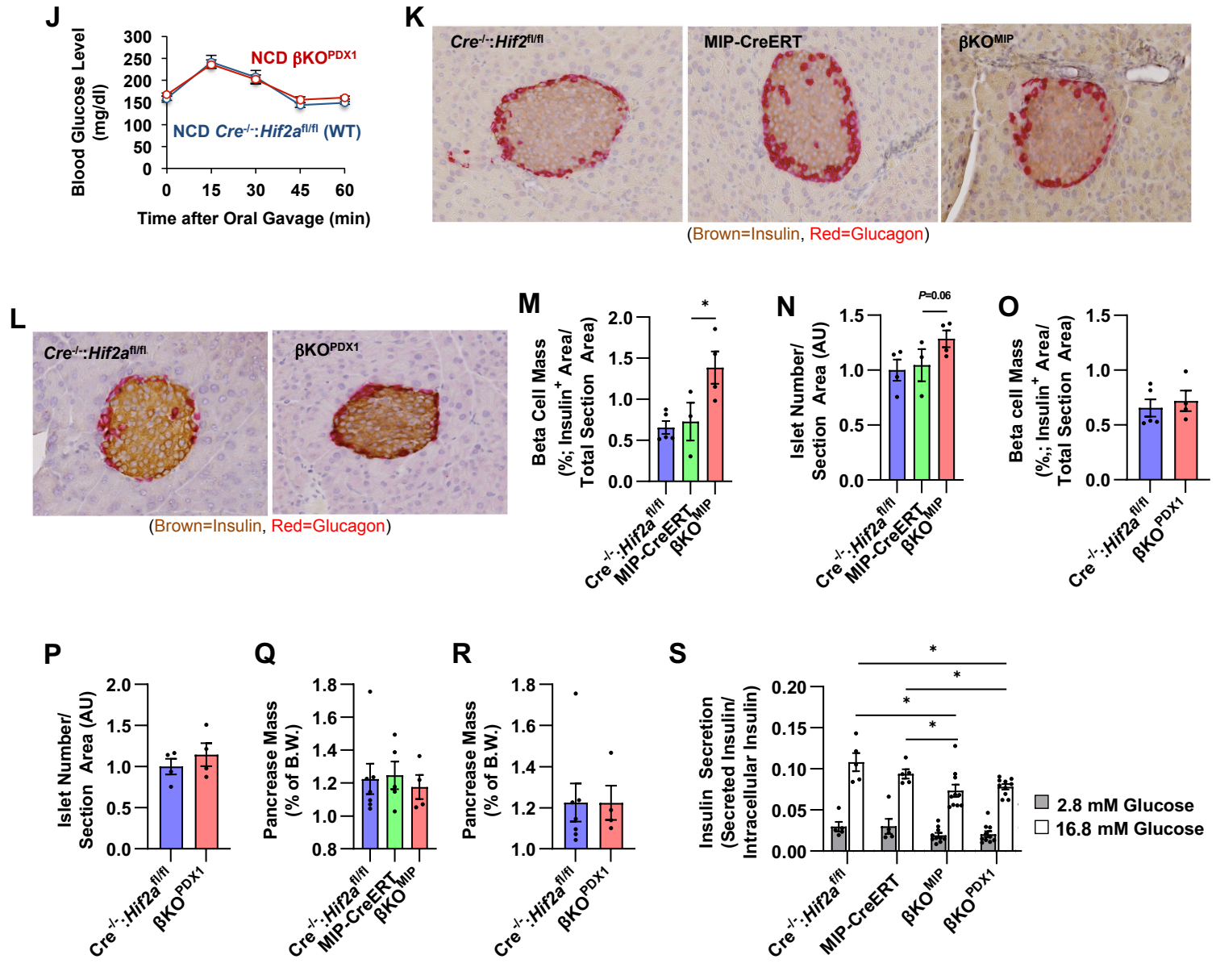

Supplementary Figure 2

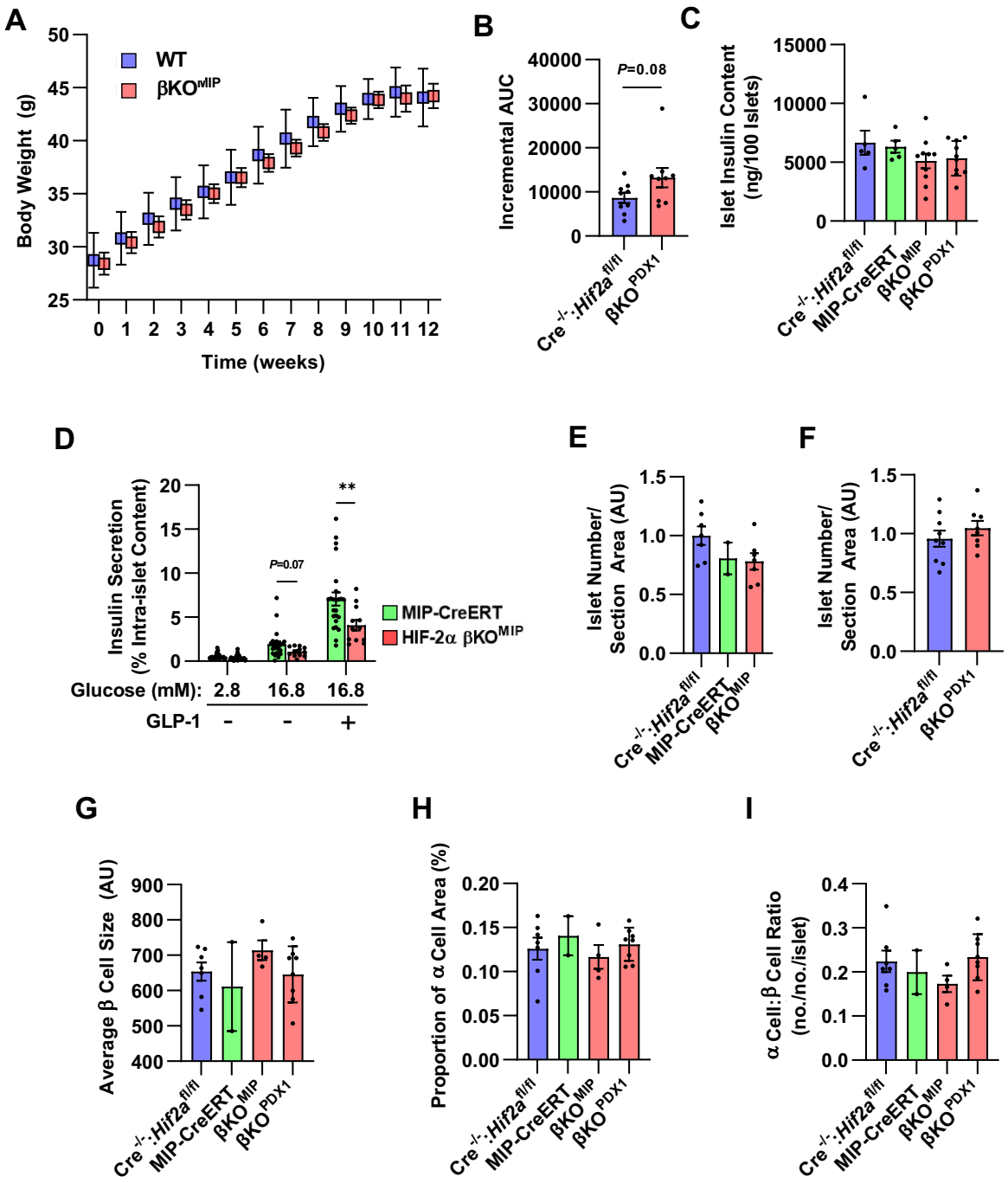

Supplementary Figure 3

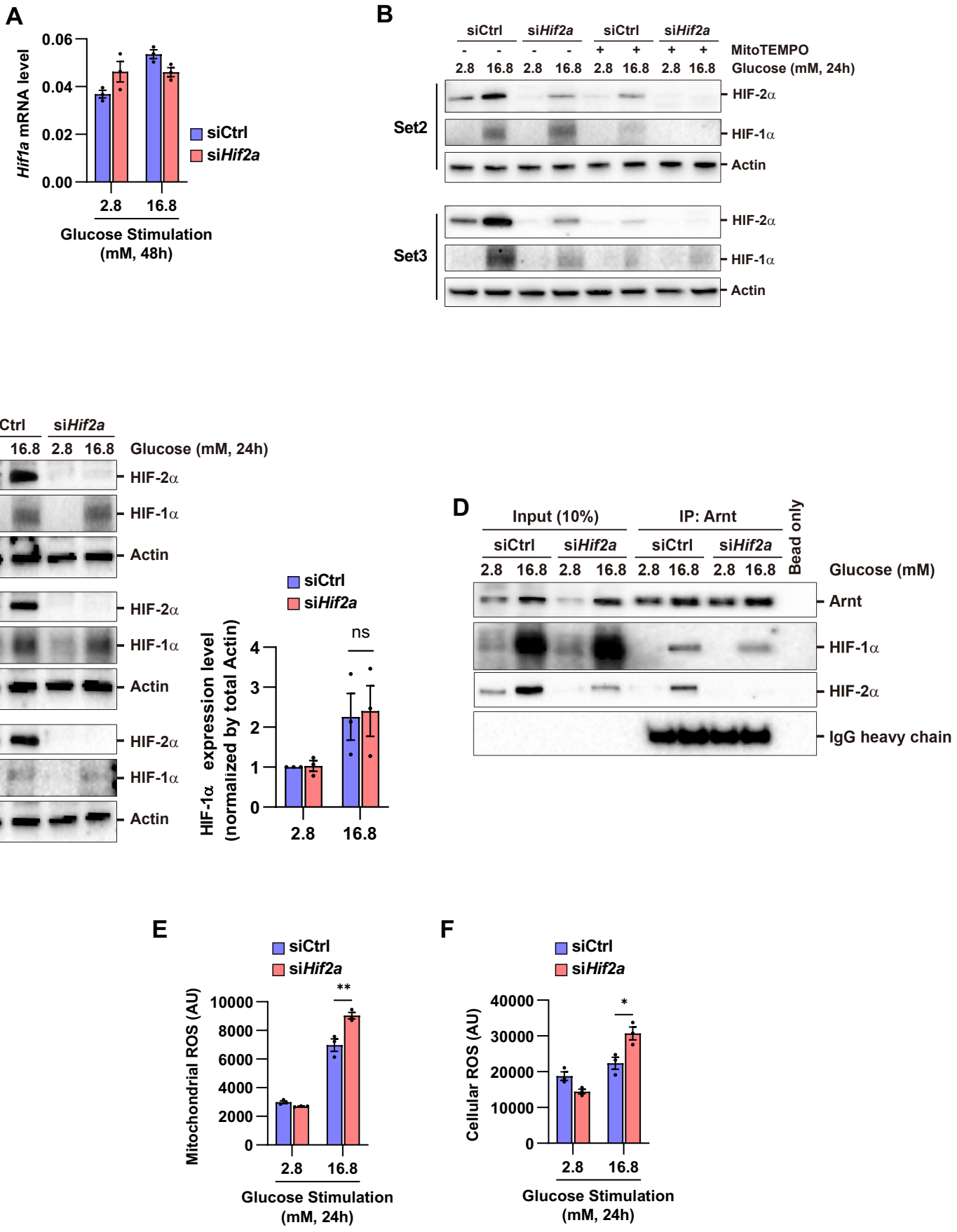

Supplementary Figure 4

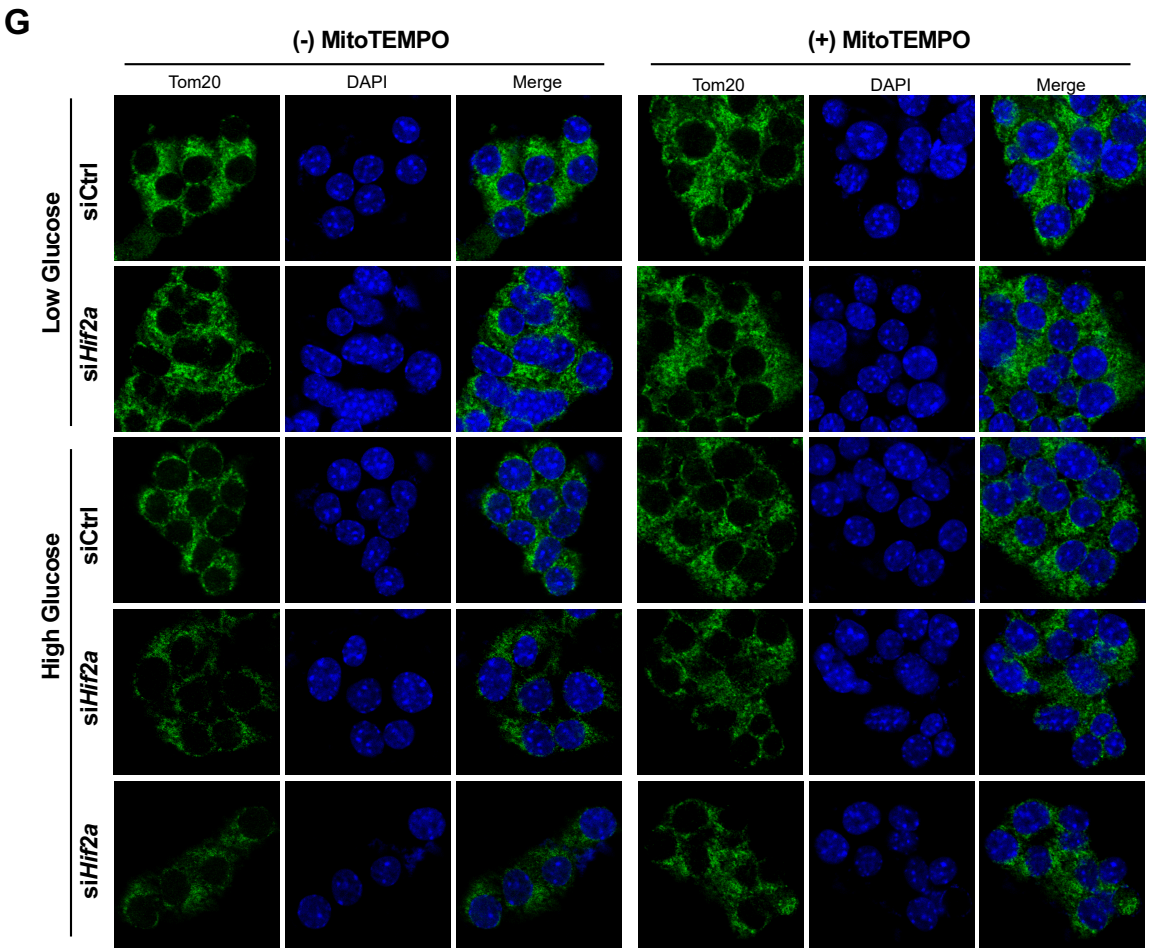

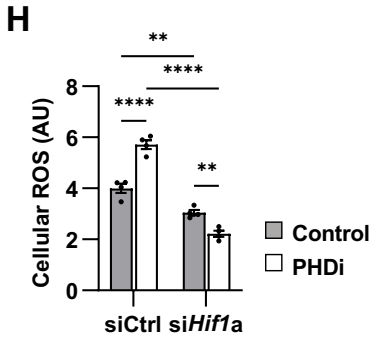

Supplementary Figure 4

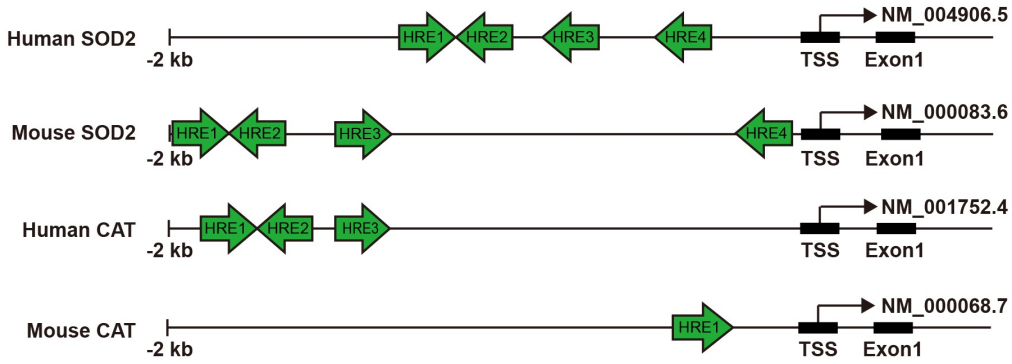

Putative HREs in human and mouse SOD and CAT gene promoters

Target	Species	Putative HRE	DNA Sequence	Position (from TSS)	Score	Strand
SOD2	Human	HRE1	GGGCGTGG	-1435 to -1427	8.29	+
		HRE2	AGGCGTGC	-1423 to -1416	8.93	-
		HRE3	CTACGTGT	-1214 to -1207	8.71	-
		HRE4	CGACGTGC	-621 to -613	10.44	-
	Mouse	HRE1	AGGCGTGT	-2124 to -2116	7.13	+
		HRE2	GGGCGTGG	-2112 to -2106	8.29	-
		HRE3	ATACGTGC	-1669 to -1661	10.27	+
		HRE4	CCGCGTGC	-26 to -18	8.57	-
CAT	Human	HRE1	AGGCGTGT	-1960 to -1952	7.13	+
		HRE2	GGGCGTGG	-1948 to -1940	8.29	-
		HRE3	AGGCGTGA	-1825 to -1817	7.35	+
	Mouse	HRE1	CGTCGTGC	-598 to -590	5.94	+

Supplementary Figure 5

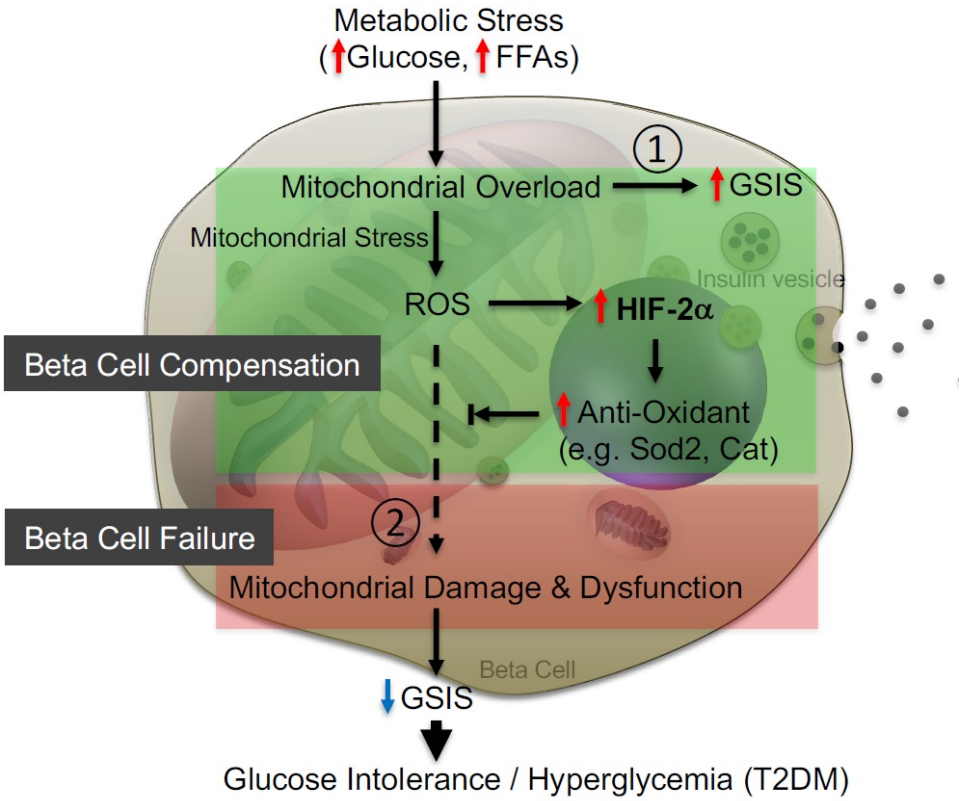

Supplementary Figure 6

Supplementary Table 1. Primers used for qRT-PCR analysis

	Genes full name	Forward primer, 5' - 3'	Reverse primer, 5' - 3'
Hif1a	Hypoxia-inducible factor 1-alpha	CAAGATCTCGGCGAAGCAA	GGTGAGCCTCATAACAGAAGCTTT
Hif2a	Hypoxia-inducible factor 2-alpha	TAAAGCGGCAGCTGGAGTAT	ACTGGGAGGCATAGCACTGT
Slc2a1	Solute carrier family 2, facilitated glucose transporter member 1	GCAGGAGTGTCCGTGTCTTC	CCTGTCTCTTCCTACCCAACC
Slc2a2	Solute carrier family 2, facilitated glucose transporter member 2	ATGTCGGTGGGACTTGTGCT	TGGACCTGGCCCAATCTCAA
Pdk1	Polycystin-1	GGACTTCGGGTCAGTGAATGC	TCCTGAGAAGATTGTCGGGGA
Ldha	Lactate dehydrogenase A	CACTGCAAGCTGCTGATCGT	CCAGCCTCTCTCCCATCAGG
Pgc1	Peroxisome proliferator-activated receptor gamma coactivator 1-alpha	GAAAGGGCCCGAGCAATCTG	TCACCAAACAGCCGGAGACT
Tfam	Transcription factor A, mitochondrial	AGCGTGCTAAAAGCACTGGG	ATAGACGAGGGGATGCGACC
Nrf1	Nuclear respiratory factor 1	AGCACGGAGTGACCCAAAC	AGGATGTCCGAGTCATCATAAGA
Nrf2	Nuclear respiratory factor 2	CTTTAGTCAGCGACAGAAGGAC	AGGCATCTTGTTTGGGAATGTG
Gpx	Glutathione peroxidase 1	CACAGTCCACCGTGTATGCC	TCAATGAGCAGCACCTTGCC
Cat	Catalase	CCAGCGACCAGATGAAGCAG	CCACTCTCTCAGGAATCCGC
Sod1	Superoxide dismutase 1	GCATGGGTTCCACGTCCATC	ACCGTCCTTTCCAGCAGTCA
Sod2	Superoxide dismutase 2	GGCCAAGGGAGATGTTACAA	GAACCTTGGACTCCCACA
Nox2	NADPH oxidase 2	CACGCATGCCTTTGAGTGGT	TGGGCCGTCCATACAGAGTC
Nox4	NADPH oxidase 4	ACCCATTTACTCTCACAATGTGTCC	GACTTGATGGAGGCAGTAGCAAAT
P47	P47 phagocyte oxidase	GATGTTCCCCATTGAGGCCG	GTTTCAGGTCATCAGGCCGC
Nos2	Inducible nitric oxide synthase	CTCAGCCCAACAATACAAGAT	TGTGGTGAAGAGTGTCATGCA
Arg1	Arginase 1	CTCCAAGCCAAAGTCCTTAGA	AGGAGCTGTCATTAGGGACAT
Pdx1	Pancreatic and duodenal homeobox 1	GAACCCGAGGAAAACAAGAGG	GTTCAACATCACTGCCAGCTC
Neurod	Neuronal Differentiation 1	GCCCAGCTTAATGCCATCTTT	CAAAAGGGCTGCCTTCTGTAA
Hnf4a	Hepatocyte Nuclear Factor 4 Alpha	ATGACACGTCCCCATCTGAAG	CTCGAGGCTCCGTAGTGTTTG
Uro3	Urocortin 3	GGAGGTCCAAGGACAAGCCT	TGCTGTGCCTGGGATTGGTA
Cx36	Connexin 36	AGTTCTCCGTCTCCCCATCTC	CCTCTAATCCGCCCTTAAGTA
Ins1	Insulin-1	GTCCTCTGGGAGCCCAAG	ACAGAGCCTCCACCAGG
Ins2	Insulin-2	ATCCTCTGGGAGCCCCGC	AGAGAGCTTCCACCAAG
36B4	60S Acidic Ribosomal Protein P0	AGATGCAGCAGATCCGCAT	GTTCTTGCCCATCAGCACC

Primers used for genotyping			
Cre	Cre recombinase	TGCAAGTTGAATAACCGGAAA	CTAGAGCCTGTTTTGCACGTT
Primer set 1		ACTCAACCTAGGGCCTTGTG	GGGAGCATTCCTGAAAAATAA
Primer set 2		ACTCAACCTAGGGCCTTGTG	GACTTACCCTCCACGACAGC
Primers used for mtDNA content assays			
mtDNA	Mitochondrial DNA	CCCAGCTACTACCATCATTCAAGT	GATGGTTTGGGAGATTGGTTGATGT
18S	18S ribosomal RNA	AGTCCCTGCCCTTTGTACACA	GATCCGAGGGCCTCACTAAAC